Purification of a Clinical Grade Recombinant Thy1-Single-Chain Variable Fragment for Molecular Imaging of Pancreatic Ductal Adenocarcinoma

Natacha JUGNIOT
Stanford University
Rakesh Bam
Stanford University
Ramasamy Paulmurugan (paulmur8@stanford.edu)
Stanford University

Research Article

Keywords: Single-Chain Variable Fragment (scFv), Enterokinase (EK), Protein Purification, Recombinant Protein, Clinical Application, Molecular Imaging, Ultrasound (US)

Posted Date: June 30th, 2021

DOI: https://doi.org/10.21203/rs.3.rs-646172/v1

Purification of a Clinical Grade Recombinant Thy1-Single-Chain Variable Fragment for Molecular Imaging of Pancreatic Ductal Adenocarcinoma

Natacha Jugniot, Ph.D.[1], Rakesh Bam, Ph.D.[1] and Ramasamy Paulmurugan, Ph.D.[1*]

[1]Department of Radiology, Molecular Imaging Program at Stanford, Stanford University, Palo Alto, CA, USA.

***Corresponding author:**
Ramasamy Paulmurugan, Ph.D.
Molecular Imaging Program at Stanford (MIPS)
Canary Center for Cancer Early Detection at Stanford
Stanford University School of Medicine
3155 Porter Drive, Palo Alto, CA 94304, USA.
Tel: 650-725-6097; Fax: 650-721-6921;
Email: paulmur8@stanford.edu

ABSTRACT

Molecular imaging using single chain variable fragments (scFv) of antibodies targeting cancer specific antigens have been considered a non-immunogenic approach for early diagnosis in the clinic. Usually, production of proteins is performed within *Escherichia coli*. Recombinant proteins are either expressed in *E. coli* cytoplasm as insoluble inclusion bodies that often need cumbersome denaturation and refolding processes, or secreted toward the periplasm as soluble proteins that highly reduce the overall yield. However, production of active scFvs in their native form without any heterologous fusion is required for clinical applications. In this study, we expressed Thy1-scFv as a fusion protein with a N-terminal sequence including 3 hexa-histidines as purification tags together with a Trx-tag and a S-tag for enhanced-solubility. Our strategy allowed to recover ~35% of Thy1-scFv in the soluble cytoplasmic fraction. An enterokinase cleavage site in between Thy1-scFv and the upstream tags was used to regenerate the native protein with 97.7 ± 2.3 % purity without any tags. Finally, Thy1-scFv showed functionality towards its target on flow cytometry assays. *In vivo* molecular imaging using Thy1-scFv conjugated to an ultrasound contrast agent ($MB_{Thy1\text{-}scFv}$) demonstrated signal enhancement on a transgenic pancreatic ductal adenocarcinoma (PDAC) model (3.1 ± 1.2 a.u.) compared to control (0.4 ± 0.4 a.u.) suggesting potential for PDAC diagnosis. Overall, our strategy facilitates the expression and purification of a clinically translatable Thy1-scFv while introducing its ability for diagnostic molecular imaging of pancreatic cancer. The presented methodology could be expanded to other important eukaryotic proteins for various applications, including but not limited to molecular imaging.

Key words: Single-Chain Variable Fragment (scFv), Enterokinase (EK), Protein Purification, Recombinant Protein, Clinical Application, Molecular Imaging, Ultrasound (US)

INTRODUCTION

Molecular imaging techniques play a central role in clinical oncology by enhancing diagnostic and therapeutic approaches. Ultrasound (US) molecular imaging (USMI) is a recent modality with greatly improved detection accuracy compared to conventional US. When using molecularly targeted US contrast agents, USMI has shown combined advantages of the US modality and molecular imaging. With the recent first molecular US contrast agent to enter clinical trials, innovation in human cancer imaging by US lies ahead. Targeted US contrast agents called microbubbles (MBs) are gas-filled microparticles synthesized by conjugating specific ligands onto the MB shell making them to bind tumor neovascular targets and enabling enhanced-tumor detection. However, producing targeted-ligands as recombinant proteins/antibodies without heterologous tags is needed to generate non-immunogenic agents for translational applications.

With the introduction of the recombinant DNA technology in 1974[1], faster, easier, and more efficient production of heterologous proteins have been performed to purifying them from natural sources. Nowadays, diverse expression systems such as bacteria, yeast, insect cells, mammalian cells, cell-free systems, transgenic animals and plants have been used for the expression of recombinant proteins. Each host system has its own merits and limitations, and plays a critical role not only in the expression of the protein of interest, but also in the way it can be subsequently purified.[2]

Escherichia coli remains the most attractive host for recombinant protein expression when considering its well understood genetics, ease of genetic manipulation, a cost effective expression, and a rapid proliferation at a high density in inexpensive growth media.[3, 4] However, as a prokaryotic system, *E. coli* may not be able to produce some eukaryotic proteins in their native form because of: (1) the complex structural features of the eukaryotic protein of interest, (2) the mRNA instability in prokaryotic system, (3) the usage of toxic codons for the host, (4) the lack of post-translational modifications, (5) the degradation of the protein by host proteases, (6) an improper folding, and (7) a poor protein solubility.[5] To overcome such issues, strategies include the use of mutated host strains, mRNA enhanced-stability, use of optimal codons, the co-expression of molecular chaperones such as foldases and post-translational protein modifying enzymes, as well as the optimization of growth conditions.[6, 7] Despite the plethora of methodologies available, challenges remain in providing recombinant proteins with relevant quantity, purity, solubility, functionality, and translatability for clinical applications (Figure 1). Periplasmic protein expression is considered a favorable approach for disulfide bond formation in *E. coli,* and was initially the most frequently used methodology.[8] Alternatively, expressing proteins in the cytoplasm leads to much higher expression level but results in aggregation into insoluble inclusion bodies (IBs).[9,10] Although it is useful in many cases where large amounts of proteins are needed, denaturation/refolding protocols of IB necessitate the use of strong denaturants and reducing agents,[11] which can lead to improper refolding, and might not give full recovery of the protein with its biological activity.[12] On the other hand, a wide range of fusion partners with solubilization tags (*e.g.,* thioredoxin (Trx), poly(NANP) (N-acetylneuraminic acid phosphatase), S-tag) are now available for enhanced expression of cytosoluble recombinant proteins, and affinity tags (*e.g.,* maltose binding protein (MBP), glutathione-S-transferase (GST), hexa-histidine tag) for more efficient purification processes.[13, 14] Although tag sequences are essential for the expression and purification of recombinant

proteins, they can interfere with the structure and function of their fusion partner while limiting their application in the clinic due to the immunogenecity. Therefore, tag removal should be considered, especially if the protein of interest is intended for clinical applications or structural studies.[15] Hence, developing protocols for the recombinant production of eukaryotic proteins in their native form is important.

With the goal of developing US contrast agent for pancreatic ductal adenocarcinoma (PDAC) imaging, we chose to express the single-chain variable fragment (scFv) targeting the thymocyte differentiation antigen (Thy1/CD90),[16] known to be overexpressed on the neovasculature of various cancers (*e.g.,* colon cancer,[17] glioblastoma,[18] hepatocellular carcinoma,[19] ovarian cancer,[20] prostate cancer[21] and PDAC[22, 23]). We have previously engineered an anti-Thy1-scFv (or simply called « Thy1-scFv ») through directed evolution of scFv protein scaffold using a yeast surface display library.[24] Here, we further engineer Thy1-scFv as a fusion protein with a N-terminal sequence including hexa-histidine tandems (1, 3 or 5 hexa-histidines) as purification tags together with a Trx-tag and a S-tag for improving solubility, and an enterokinase (EK) cleavage site at the junction of Thy1-scFv and the upstream tags for tag removal. We choose the extensively used Δgor, ΔtrxB, DsbC$^+$ SHuffle T7 *E. coli* system to express the engineered protein with disulfide bonds in the cytoplasm. The method we describe here stands out for its efficacy and relative simplicity to produce Thy1-scFv using complementary tag sequences (Figure 2) which, when cleaved using EK, resulted in generating the native Thy1-scFv without any tag. The evaluation of native-Thy1-scFv showed successful receptor binding capacity *in vitro*, promising for its use in diagnostic molecular imaging of PDAC. Our *in vivo* results illustrated the conserved functionality of Thy1-scFv enabling PDAC molecular imaging by US. The presented method can be beneficial at the outset of many project implying eukaryotic protein production for translational clinical applications.

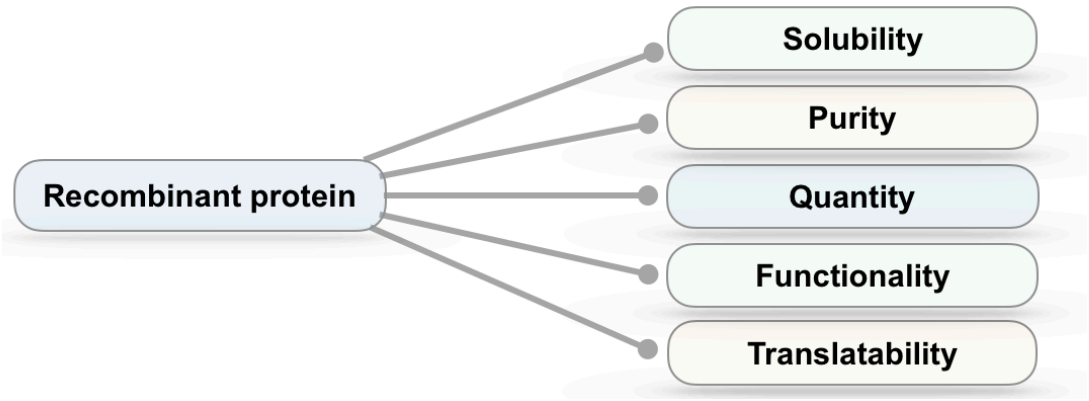

Figure 1. Recombinant protein checkpoints.

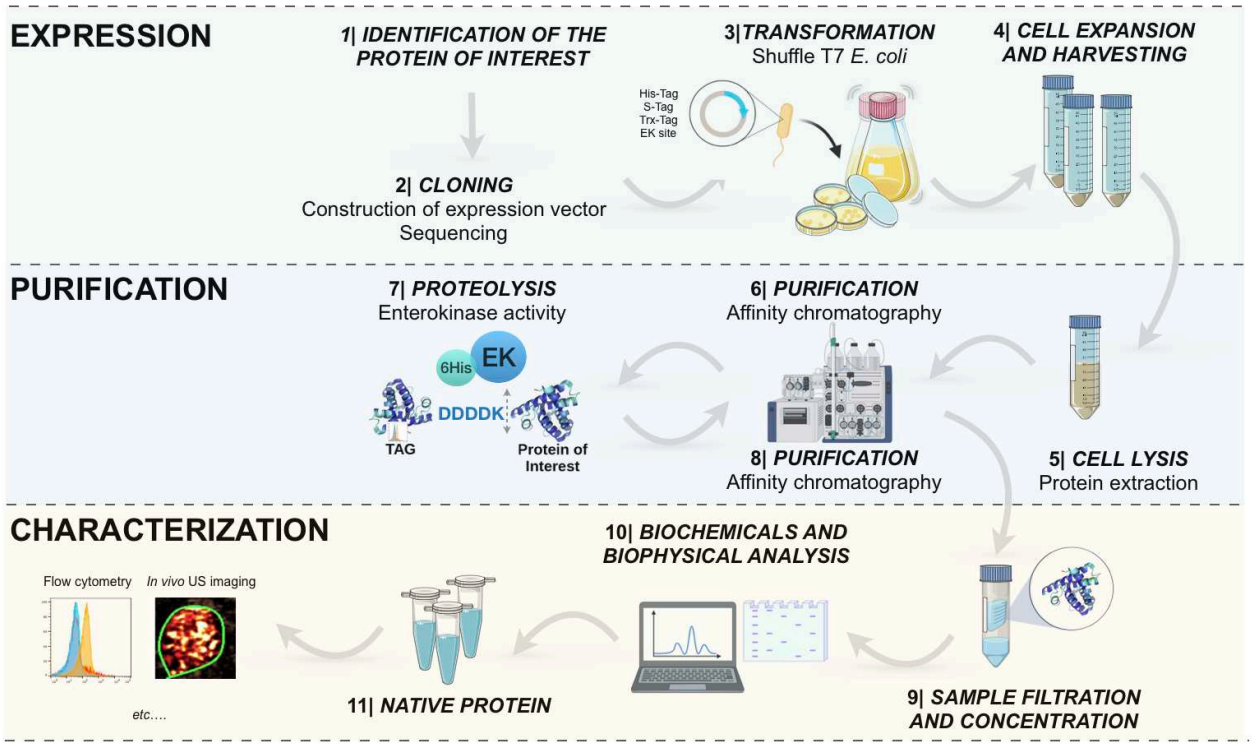

Figure 2. Schematic workflow showing the methodology employed for the construction, expression and purification of recombinant protein in its native form.

RESULTS

Engineering, expression and purification of Thy1-scFv

Construction of vectors expressing Thy1-scFv gene for efficient soluble protein production

We constructed three different expression vectors in the popular pET32b vector backbone with Trx- and S-tags and additional tandem His-Tags, giving: pET32b-1XHis-scFv, pET32b-3XHis-scFv, and pET32b-5XHis-scFv (Figure 3a). Sequence confirmed, clones were transformed into T7 SHuffle *E. coli* cells to investigate the effect of each variants on the expression and purification of Thy1-scFv. In all constructs, the tagged-Thy1-scFv has a theoretical molecular weight of around 50 kDa.

Optimization of conditions for Thy1-scFv expression and purification

Protein expression in *E. coli* was induced at 30°C (Figure 3b; Supplementary Figure S1) since higher temperatures usually result in a rapid decrease in protein yield due to degradation and misfolding.[26] As expected, at 37°C, the expression rate of Thy1-scFv was very low (Supplementry Figure S2), in contrast, we observed an increase in our target protein yield when cultured at 30°C probably because such lower temperature reduces protein degradation, improves folding efficiency, and thus reduces IB formation. Moreover, endogenous proteases have a higher turnover rate when *E. coli* is grown at 37°C, thus leading to an enhanced-proteolysis of Thy1-scFv into a Thy1-scFv fragment (around 25 kDa). We detected Thy1-scFv at an apparent molecular weight, which was consistent with its theoretical mass in all three constructs. Importantly, culture expressing the construct pET32b-3XHis-scFv with an induction temperature of 30°C showed higher protein level compared to the other constructs (Figure 3b, pET32b-3XHis-scFv, lanes 6 to 8), and Thy1-scFv was isolated with 47.7± 11.5 % purity. This is in part due to higher binding of Ni-agarose with the 3X-His-tag used for purification. Apart from the full length Thy1-scFv, a fragment of around 25 kDa was the major co-purified protein. We suspected it to come from residual endogenous proteolytic activity on Thy1-scFv on a locally weaker structure probably in the multi-histidine tag region. After transfer onto a PVDF membrane, an anti-hexa-histidine tag antibody was used to confirm the presence of Thy1-scFv. Analysis of both soluble and insoluble fractions indicates that ~35% of the protein can be recovered in the soluble fraction (Supplementry Figure S3). The tagged-scFv from pET32b-1XHis-scFv binds the column with weak affinity and therefore is co-purified with many contaminants. The use of pET32b-5XHis-scFv generates a longer and more flexible tag sequence, more prone to reach protein binding sites and improper column binding as suggested by the elution profile. Based on these results, the construct pET32b-3XHis-scFv was chosen. Fractions 6 to 8 from this construct were pooled and used for further enrichment. Elimination of imidazole salts resulted in a more stable protein, and the sample was concentrated (Figure 4, undigested T_0) yielding to 0.37 ± 0.15 mg of tagged-Thy1-scFv per liter of bacterial culture (Table 1), difficult to reach using more conventional method of purification.

Optimization of tag removal by enterokinase activity

To optimize the hydrolysis efficacy of EK on the fusion protein, 30 µg of the purified tagged-protein were incubated with 0.5, 1, 2 and 8 Unit(s) of EK at 25°C for different times (1, 4, 8 and 24 hour(s)) (Figure 4). Incubation of the tagged-Thy1-scFv with EK resulted in the generation of native scFv (~ 30 kDa; expected

molecular weight 27,936 Da) and free tags (~ 17 kDa). Product bands appeared in all conditions after 1h incubation along with undigested substrate. After 4h, the substrate is almost completely digested (approximately 80% of full length fusion protein was cleaved with 1, 2 and 8 U, Supplementry Figure S4a). However, an incubation time > 4 h or the use of ≥ 8 U of EK during a time > 1 h triggers non-specific cleavage of Thy1-scFv (Supplementry Figure S4b) and is also not cost effective. No spontaneous hydrolysis was detected after 24 h of incubation.

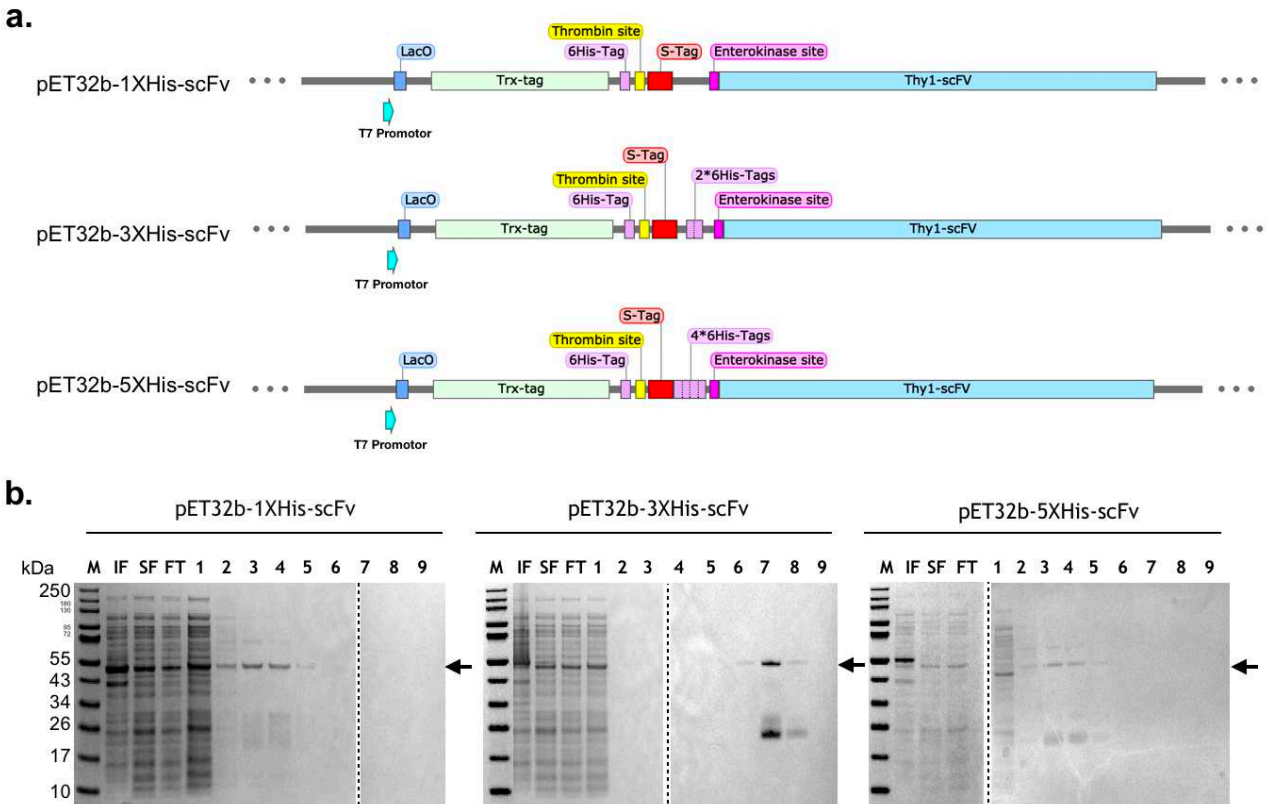

Figure 3. Construction and expression of recombinant Thy1-scFv proteins. **(a)** Schematic map showing the cloning pattern of pET-32b vector constructed to express recombinant Thy1-scFv in various formats (different number of hexa-histidine tags): pET32b-1XHis-scFv, pET32b-3XHis-scFv, and pET32b-5XHis-scFv. **(b)** Purity of protein based on the elution fraction: Thy1-scFv formats resolved in 4-12% gradient SDS-PAGE. M: protein molecular weight marker; IF: insoluble fraction from cell lysate; SF: soluble fraction from cell lysate; FT: flow through; lanes 1-9: eluted fractions; arrows indicate the position of the tagged-Thy1-scFvs. The same methodology was applied for all Thy1-scFv formats and gels were processed in parallel. Dotted lines have been used to delineate different gels. Full-length gels are presented in Supplementary Figure S1.

Native Thy1-scFv purification

Following a second immobilization by metal affinity chromatography, 0.22 ± 0.11 mg of native scFv can be recovered with 97.7 % purity (Figure 5a, lane FT). Additional mass spectrometry analysis highlighted a prominent species of scFv monomer (m/z = 27,582) with a small fraction of dimer (m/z = 55,505) (Figure 5b). Contrary to the first purification round (Figure 6a) where the recombinant protein was recovered in the latest elution fractions, the native protein was isolated in the flow through fraction (Figure 6b). Recombinant EK, uncleaved recombinant Thy1-scFv and fragments containing histidine tags were retained on the column.

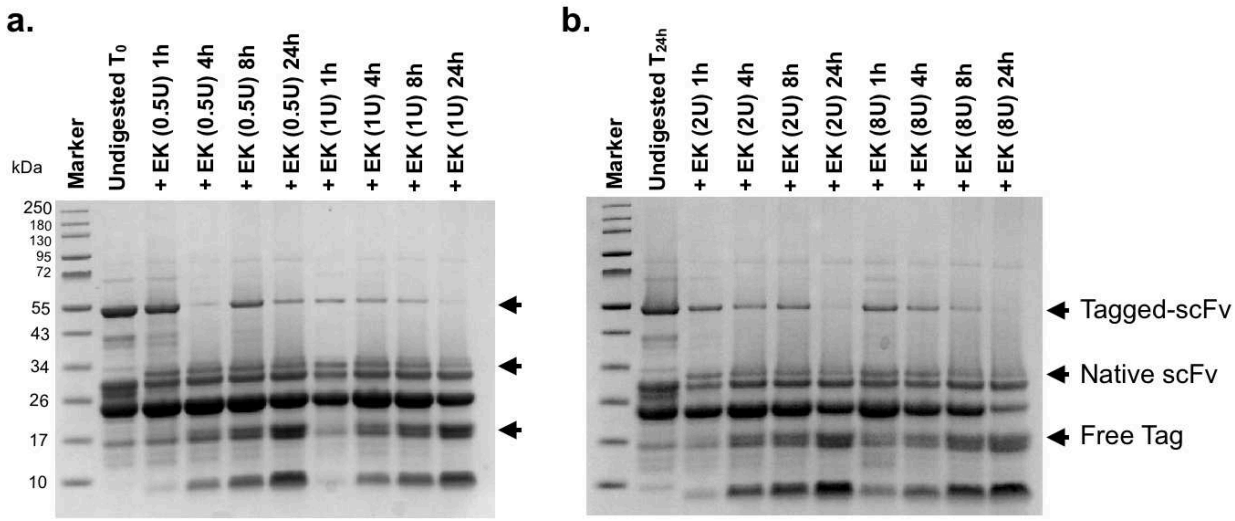

Figure 4. Optimization of EK incubation time and concentration from **(a)** 0.5U and 1U to **(b)** 2U and 8U, for tag removal of the recombinant Thy1-scFv protein. Gels were processed in parallel.

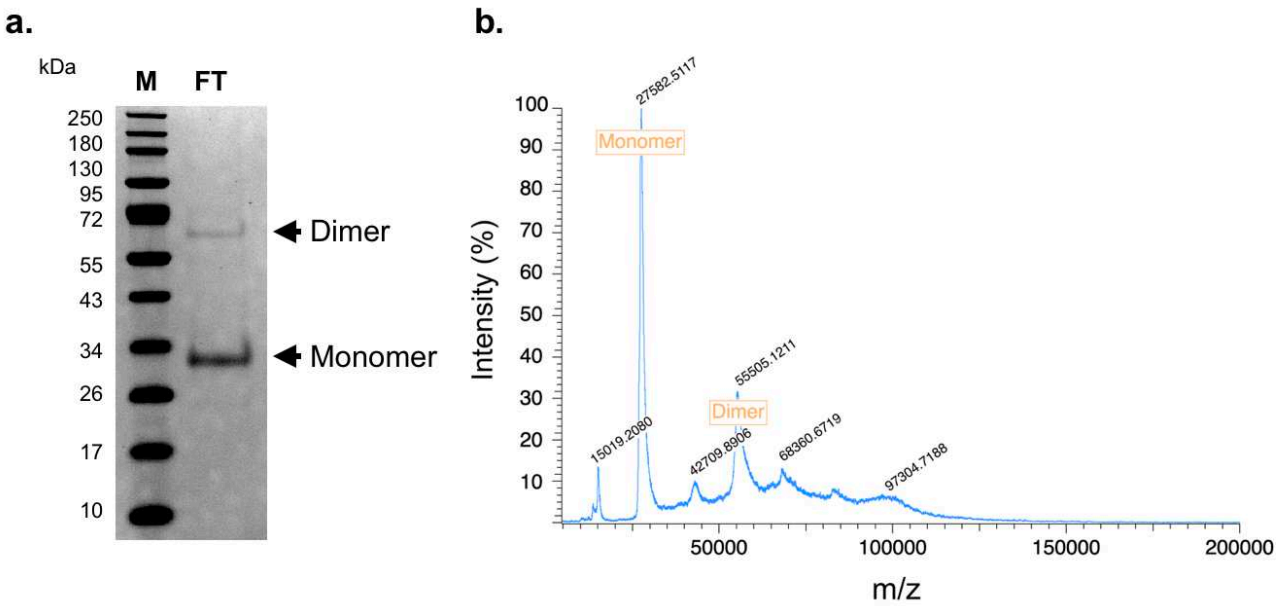

Figure 5. Second step purification of Thy1-scFv after proteolysis. (a). Gel electrophoresis showing the native Thy1-scFv. M: protein molecular weight marker; FT: flow through. (b). Mass spectrometry on Thy1-scFv flow through fraction.

Thy1-scFv binds to Thy1 expressing cells *in vitro*

APC conjugated commercial antibody (Thy1-Ab-APC) was used as positive control to confirm cell-surface expression of Thy1 (Figure 7). Binding capacity of Thy1-scFv-APC was performed against both Thy1 expressing cells ($MS1_{Thy1}$) and control cells ($MS1_{WT}$) by flow cytometry. Incubation of cells with Thy1-scFv-APC showed higher binding to $MS1_{Thy1}$ compared to the controls as detected by a shift toward

increased fluorescent signal intensity. Thus, the recombinantly expressed Thy1-scFv retained its ability to bind to its target cells *in vitro*.

Purification step	Volume (mL)	$[Proteins]_{total}$ (mg/mL)	Total proteins (mg)	Tagged-Thy1-scFv purity (%)*	Native Thy1-scFv purity (%)*	Tagged-Thy1-scFv (mg)	Native Thy1-scFv (mg)
Cell lysate (n=5)	20	27.2 ± 4.6	543 ± 92	-	-	-	-
IMAC1 (n=5)	1.1 ± 0.3	0.69 ± 0.1	0.78 ± 0.2	47.7 ± 11	-	0.37 ± 0.1	-
IMAC2 (n=3)	1.2 ± 1.1	0.15 ± 0.04	0.23 ± 0.1	-	97.7 ± 2.3	-	0.22 ± 0.1

Table 1. Summary of Thy1-scFv purification from 1L bacterial culture. *value based on analysis of Thy1-scFv band intensity using BioRad Gel-Doc system.

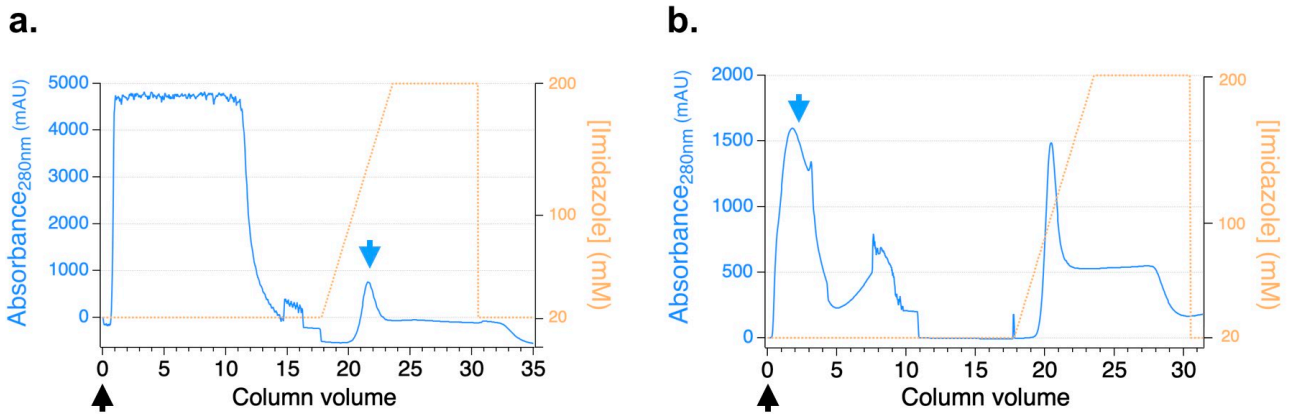

Figure 6. Elution profile of Thy1-scFv on Ni-NTA IMAC. **(a)** IMAC1: tagged-Thy1-scFv is collected during the elution step. **(b)** IMAC2: native Thy1-scFv is collected in the flow through fraction. Black arrows represent the time of injection, and blue arrows indicate the peak and elution time of the protein of interest.

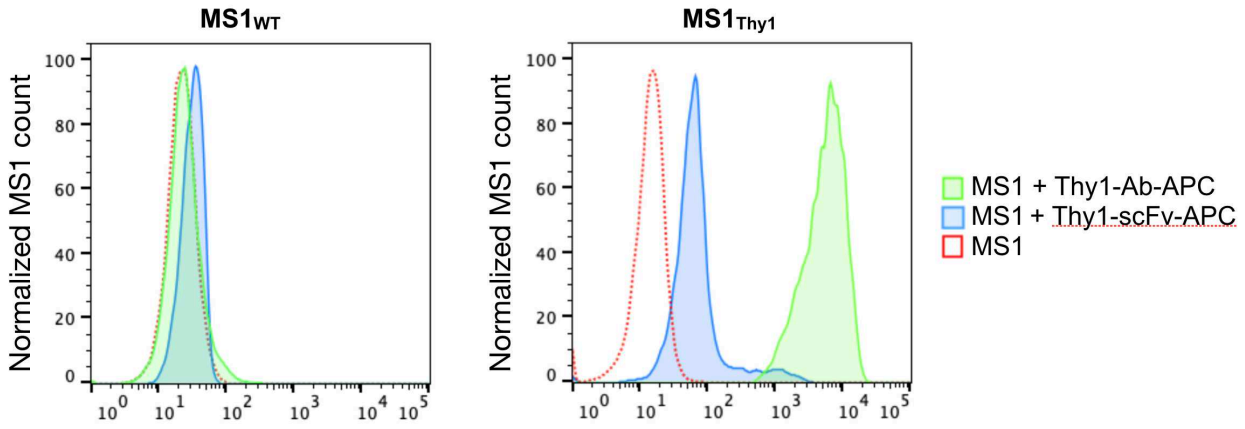

Figure 7. Binding efficiency of Thy1-scFv to MS1 cells.

***In vivo* US contrast agents functionalized with Thy1-scFv enhance PDAC neovasculature imaging in transgenic animal model of spontaneous PDAC**

To test the *in vivo* functionality of Thy1-scFv, we used US contrast agents (MBs) harboring Thy1-scFv on their surface using NHS-chemistry, giving $MB_{Thy1\text{-}scFv}$. Control MBs without ligand were reported as $MB_{non\text{-}targeted}$. Prior to imaging, both MB types were tested for size and concentration changes that may occur due to Thy1-scFv's influence on steric changes or gas dissipation.

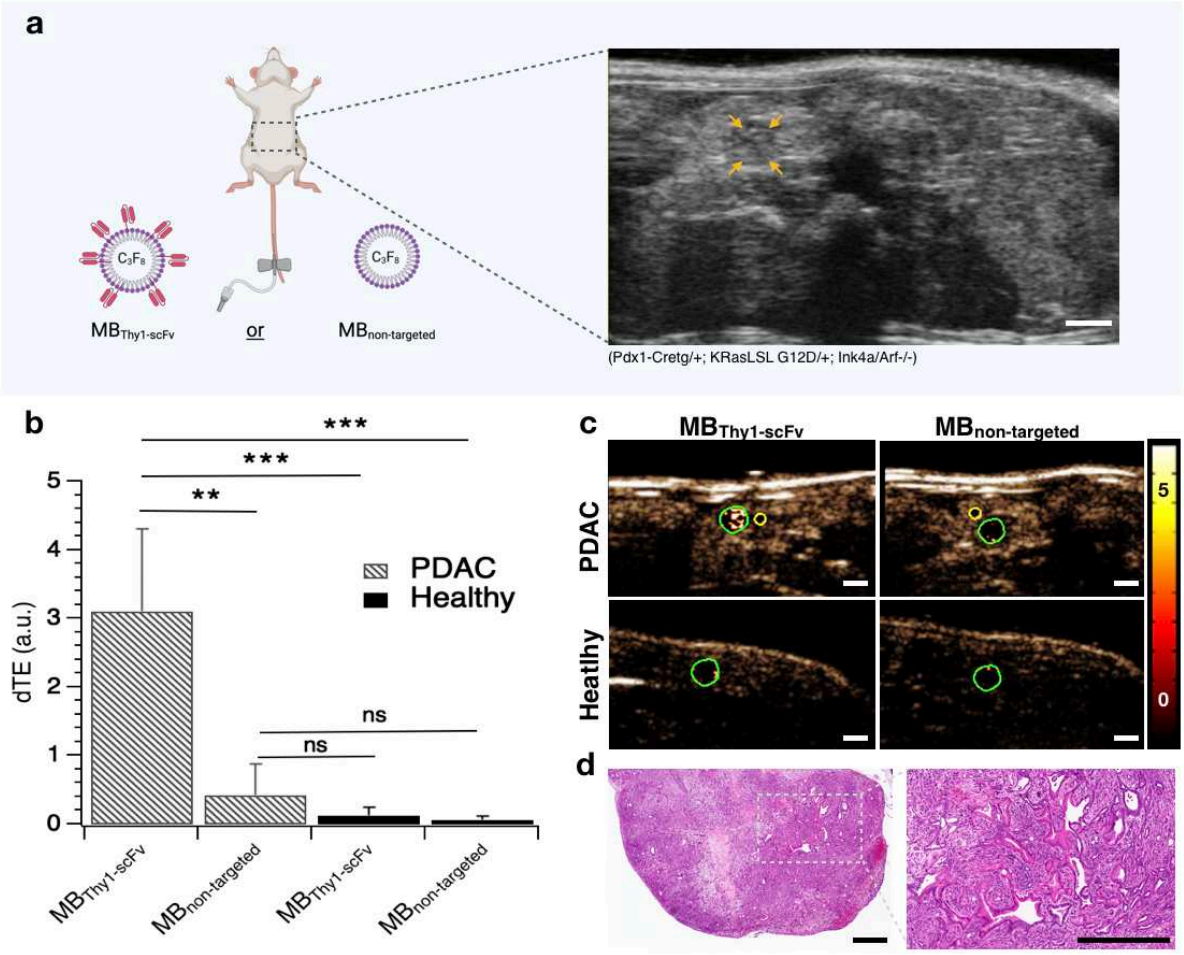

Figure 8. *In vivo* US molecular imaging of Thy1 in genetically engineered transgenic mouse model with spontaneous PDAC. **(a)** Schematic illustration of overall experiment. $MB_{Thy1\text{-}scFv}$ and $MB_{non\text{-}targeted}$ were successively tested for Thy1 binding in transgenic mouse model of PDAC after tail vein injection of contrast MBs (left) and representative B-mode abdominal image of PDAC-transgenic mouse (right). Orange arrows delineate a pancreatic tumor. B-mode images were used as a reference to draw ROIs in contrast-mode images in 'c'. Scale bar = 1 mm; **(b)** Quantitative bar graphs of *in vivo* signal enhancement (dTE) using targeted and non-targeted contrast agents in PDAC and healthy mice. **, $P < 0.03$; ***, $P < 0.02$; **(c)** Representative transverse contrast-mode US images showing stronger signal enhancement in PDAC (green ROI) after injection of $MB_{Thy1\text{-}scFv}$, and only low signal following injection of $MB_{non\text{-}targeted}$. Background signal was noted in adjacent normal pancreas (a yellow ROI was drawn to quantify imaging signal in adjacent non-PDAC tissue). Scale bar = 1 mm; color coded scale is shown for US molecular imaging in arbitrary units (a.u.). **(d)** Corresponding hematoxylin-eosin-stained sample confirms presence of PDAC in transgenic mouse model. Scale bar = 500 μm.

The incorporation of Thy1-scFv as part of the MB composition, *i.e.,* $MB_{Thy1\text{-}scFv}$, did not affect the MB mean diameter or the size distribution compared to $MB_{non\text{-}targeted}$ (mean diameter = 1.2 ± 1.4 µm and 1.1 ± 0.8 µm, respectively) nor the concentration (1.10^9 particles/mL and $1.2.10^9$ particles/mL, respectively) in agreement with MBs used in the clinic (*e.g.,* Definity (Lantheus Medical Imaging), Sonovue (Bracco Diagnostics)) (Supplementary Figure S5). Tumors were located on B-mode imaging and MBs were injected intravenously (Figure 8a). On contrast mode, mice injected with $MB_{Thy1\text{-}scFv}$ showed tumors with significantly increased Thy1 molecular imaging signal (3.1 ± 1.2 a.u.) compared to $MB_{non\text{-}targeted}$ (0.4 ± 0.4 a.u.), with a quantitative outcome of ~7.8-fold ($p<0.03$) (Figure 8b and c) compared to control. Conversely, imaging of healthy pancreas did not produce any significant differences in imaging signal between the two MB constructs ($MB_{Thy1\text{-}scFv}$ = 0.1 ± 0.1 a.u. and $MB_{non\text{-}targeted}$ = 0.07 ± 0.06 a.u) and were significantly lower than with $MB_{Thy1\text{-}scFv}$ in PDAC model (39-fold, $p<0.02$). Histological analysis of H&E-stained tissues confirmed presence of PDAC (Figure 8d). Overall, these results demonstrate conserved Thy1-targeting property of Thy1-scFv *in vivo,* and sketches the applicability for PDAC US molecular imaging.

DISCUSSION

Molecular imaging has made a considerable contribution to oncology throughout the course of early detection and prognosis, and is an integral part of clinical trials. Biomarkers can be detected with various targeted-probes based on antibodies, peptides or proteins, oligonucleotides, or small molecules conjugated to imaging agents for suitable imaging modalities. Specifically, recombinant protein expression has become an established technique for efficient production of cancer specific antigen-binding ligands in bacterial systems. However, conventional methods can be cumbersome toward meeting criteria for clinical applications. The purpose of this study was to engineer an efficient production model for clinical grade recombinant proteins through the example of Thy1-scFv, while introducing its potential for early diagnostic of pancreatic cancer.

In vitro refolding technology of IBs has became prevalent to recover insoluble eukaryotic proteins expressed in *E. coli*.[10, 27] IBs are usually denatured with high concentration of chaotropes such as urea or guanidine hydrochloride.[28] The major drawbacks of this method are its complex and expensive operational process, which further needs optimization at multiple steps. In addition, use of high concentrations of denaturing agents results in complete denaturation of the secondary structure favoring re-aggregation during successive process.[27] Thus, recovery of soluble and active protein can be greatly reduced. In this study, we proposed an alternative to such extreme procedures and presented a multi-step process for enhanced-soluble protein production in SHuffle T7 *E. coli* cells cytoplasm using the gene fusion technology. We used the well known Trx-tag, improving disulfide bond formation, combined with S-tag. S-tag, commonly used as affinity tag, was here employed to enhance Thy1-scFv solubility thanks to its abundance in charged and polar residues.[29] Both Trx-tag and S-tag are small and do not interfere with the proper folding or function of a fused target protein. Although essential for the expression and purification of recombinant proteins, tag sequences have the potential to interfere with the structure and the function of their fusion partner. In addition, many tags have interacting partners in mammalian system which can interfere with the biological applicability of

recombinant proteins while generating a strong immune reaction. Therefore, tag removal should be considered, especially if the target protein is intended for pharmaceutical or therapeutic clinical applications, for crystallization, and for structural determination studies.[15] Chemical cleavage methods are usually inexpensive[30] but most systems rely on endopeptidases to separate the fusion partner from the protein of interest.[31] Serine proteases such as the activated blood coagulation factor X (Factor Xa), EK, thrombin, have been used, as well as viral proteases such as tobacco etch virus (TEV) protease and rhinovirus 3C protease. Viral proteases have a more stringent sequence specificity due to their much slower turnover rates (catalytic rate constant (kcat)),[32-36] however EK has no amino acid specificity requirement on the P' part of the scissile bond (DDDDK↓) (only proline and tryptophan should be avoided on P1' which corresponds to an alanine residue in our study). Consequently, when an affinity tag is joined to the N-terminus of the protein of interest, EK is able to regenerate a native N-terminus. Moreover, we used a recombinant EK presenting the same affinity tag attached to the protein of interest, *i.e.*, hexa-histidine tag. This allowed to apply the digestion products on the same affinity chromatography for separation. Undigested fusion protein substrate, tagged-protease, cleaved tag, and any endogenous proteins that bound to the affinity resin will be separate from the untagged protein of interest in the unbound effluent. After removal of the fusion partner tag, the native Thy1-scFv was recovered in good quantity (0.22 mg ± 0.11). Its binding functionality was proved *in vitro* on Thy1-expressing cells, and in transgenic animals. Based on our results, we anticipate that the vector design and basic strategy presented in this study should be applicable to many proteins of biological interest which are currently difficult to purify. Overall, it is generally assume that for *E. coli*, a 1-liter fermentation will generate ~ 150 mg of total cellular proteins. Assuming an average yield between 0.5% to 5% of total proteins, 0.75 to 7.5 mg of recombinant protein is available in the cells. If we assume, based on our results, that protein of interests can be recovered between 30% and 50% in the soluble fraction, hence, our strategy could allow convenient small-scale production of proteins in sufficient quantities to initiate most studies (0.1 to 3 mg). Scale of production could be expanded by establishing a large-scale fermentation system to produce higher amount of proteins.

Given the low median survival rate (5-year survival rate < 9%) and the low percentage of PDAC patients qualifying for tumor resection (10-20%), the need for early screening methods is globally recognized.[37] Efforts have been made to develop molecular imaging probes capable of detecting early stage PDAC.[38] Here, we produced a clinically translatable Thy1-scFv conjugated-US contrast agent, $MB_{Thy1\text{-}scFv}$, and illustrated its potential for non-invasively enhancing US contrast between PDAC and normal pancreatic tissues in mice consistent with related findings.[24,39] Our probe, able to detect small foci in the pancreas (>2 mm), constitutes a promising translatable US molecular imaging agent. Naturally, the reproducibility and the sensitivity for PDAC molecular imaging will have to be further analyzed. This will be, however, outside the scope of this article. With the success of the first and, to date, only targeted-MB in clinical trials for various cancer, BR55 (kinase insert domain receptor-targeted peptide), a rapid expansion of targeted US contrast agents is expected. Our promising pre-clinical results with $MB_{Thy1\text{-}scFv}$ could provide opportunities for improved PDAC prognosis, and our targeted US contrast agent, a variable format for other biomarker targeting.

MATERIALS AND METHODS

Ethical approval

The Administrative Panel on Laboratory Animal Care of Stanford University approved all procedures using laboratory animals used in this study and all experiments were conducted in accordance with the Guidelines for the Care and Use of Laboratory Animals. This study was carried out following the ARRIVE guidelines.

Expression vector design

The expression vectors pET32b-1XHis-scFv, pET32b-3XHis-scFv, and pET32b-5XHis-scFv were constructed for Thy1-scFv expression. A ligation substrate featuring Thy1-scFv protein was amplified by PCR using a forward primer with *NcoI* restriction enzyme site and a reverse primer with *XhoI* restriction enzyme site. The amplified fragment was digested with *NcoI* and *XhoI* and ligated into pET-32b(+) prokaryotic expression vector digested with respective restriction enymes to construct pET32b-1XThy1-scFv with a single inherent hexa-histidine-tag located between the Trx- and S-tags. To introduce more hexa-histidine-tags to construct pET32b-3XHis-scFv and pET32b-5XHis-scFv vectors, we inserted annealed forward and reverse primers coding for 2 and 4 additional hexa-histidine-tags (*i.e.,* 3XHis and 5XHis total) with *BglII* restriction enzyme site on both the sides as overhangs with 5'- phosphate group. After ligation into pET32b-1XThy1-scFv vector previously digested with *BglII* restriction enzyme and dephosphorylated using Calf intestine alkaline phosphatase, we generated two additional vectors with 3X and 5X hexa-histidine-tags. All three plasmids contain: a T7 promotor; two fusion partners Trx- and S-tags for enhancing protein folding and solubility; 1, 3 or 5 hexa-histidine tag(s) for purification by immobilized metal affinity chromatography (IMAC); a DDDDK sequence on the N-terminus of Thy1-scFv for tag removal using EK cleavage; and the Thy1-scFv gene. Each histidine tags were separated from each other by a few amino acid residues to increase a flexible folding. The sequence confirmed, vectors were transformed into SHuffle T7 *E. coli* cells (New England Biolabs, Ipswich, MA) for recombinant protein expression. Oligonucleotides and recombinant protein sequences used in this study for constructing the vectors are listed in Supporting Information (Supplementry Table S1).

Thy1-scFv expression

Bacterial transformation was performed for each expression vector as follows: 50 µL of SHuffle T7 *E. coli* competent cells were transformed with 1 µg of expression plasmid using standard heat-shock procedure; 300 µL SOC growth media was then added in each vial for cell recovery. Cells were grown at 30°C for 1 h in a shaking incubator (100 r.p.m.), and plated on Lysogeny Broth (LB)-agar medium containing ampicillin (50 µg/ml). After overnight growth, one fresh-picked colony was inoculated in 2 mL LB-ampicillin medium (50 µg/ml) and grown overnight at 30°C (250 r.p.m.). Bacteria were transferred into 1 L of LB-ampicillin medium and further cultured until the OD_{600nm} reaches 0.4. The culture was induced for protein expression by the addition of isopropyl-β-d-thiogalactoside (IPTG, 1 mM) after diluting with the addition of one-fourth volume of pre-warmed LB-ampicillin medium. Induction was allowed for 4h at 30°C (250 r.p.m.). The pellet was then harvested *via* centrifugation (5,000 g, 10 mins, 4°C) and stored at -80 °C.

Fusion protein purification (IMAC1)

Cell pellets were resuspended in 20 mL of ice-cold lysis buffer (3 mM monosodium phosphate, 50 mM disodium phosphate, 500 mM NaCl, 5 % glycerol (v/v), 5 mM CHAPS, and 20 mM imidazole containing protease inhibitors (Thermo Scientific, Rockford, IL)) and lysed by sonication (60% amplitude, 5 s on/off, 10 cycles, Branson SLPe). The soluble and insoluble fractions were then separated by centrifugation (12,000 g, 10 min, 4°C). Insoluble fractions containing cell debris and possible IBs were washed with 8 mL of the same lysis buffer. The soluble fractions were applied to a 1 mL FF His-trap column (GE Healthcare Biosciences, PA) in an AKTA FPLC system (GE Healthcare Biosciences) equilibrated with PBS buffer containing 20 mM imidazole to reduce non-specific binding. The tagged-Thy1-scFv was purified using a linear gradient of imidazole (from 20 mM to 200 mM) in PBS buffer at a flow rate of 1 mL/min. Concentration of proteins were measured by UV spectrometry in each fraction. Purity of the fractions was analyzed on 4-12% gradient SDS-PAGE followed by staining with Coomassie Blue (SimplyBlue SafeStain, Carlsbad, CA) for visualization using a BioRad Gel-Doc system. Fractions containing the protein of interest were pooled and the best expression vector was utilized for further experiments. Western blot analysis was performed using anti-His tag antibody. The insoluble and soluble fractions resolved in 4-12% gradient SDS-PAGE gel were electroblotted onto a polyvinylidene difluoride (PVDF) membrane, blocked in PBS-T (PBS with 0.05% Tween 20) with 5% milk powder for overnight at 4°C and then treated with anti-His tag antibody (BioLegend, San Diego, CA). After washing, the membrane was incubated with HRP-conjugated anti-mouse IgG antibody. Signals were visualized by the addition of enhanced-chemiluminescence (ECL) substrate and imaging using IVIS *in vivo* imaging system (Perkin Elmer, Santa Clara, CA).

Fusion protein cleavage by enterokinase

The purified protein was further treated with EK to remove the overhang tags (trx, S-tag and His-tags). Before EK treatment, the protein solution containing PBS-imidazole buffer was exchanged with 10 mM Tris HCL, 300 mM NaCl, pH7.4, using a 30-kDa molecular weight cutoff Vivaspin Protein Concentrator Spin Column (GE Healthcare Lifesciences, Pittsburgh, PA). In addition, the sample was concentrated during the same step. Tag removal was performed using EK enzyme tagged with hexa-histidine (Genscript, Piscataway NJ; MW = 22.7 KDa) ranging from 10 to 160 IU per milligram of protein during 1h to 24h incubation period at 25°C. Optimal EK concentration and incubation time were used for further experiments.

Purification of native protein (IMAC2) and characterization for purity

Following EK mediated cleavage, the sample was loaded on the equilibrated 1 mL FF His-trap column. Thereafter, the flow through was collected, followed by the application of a linear gradient of PBS buffer containing imidazole ranging from 20 mM to 200 mM. The fractions were collected and examined for Thy1-scFv purity and size by Matrix-Assisted Laser Desorption/Ionization time-of-flight (MALDI-TOF) mass spectrometry and SDS-PAGE. Fractions containing the native Thy1-scFv were pooled and further desalted/ concentrated using a 10-kDa molecular weight cutoff Vivaspin Protein Concentrator Spin Column (GE Healthcare Lifesciences, Pittsburgh, PA) with PBS buffer, pH 7.4.

Cell culture

Wildtype MILE SVEN 1 ($MS1_{WT}$) mouse vascular endothelial cells (CRL2279; American Type Culture Collection (ATCC)) and MS1 cells engineered to stably express human Thy1 protein ($MS1_{Thy1}$) (selected using puromycin antibiotic marker) were cultured under sterile conditions in Dulbecco's Modified Eagle Medium (DMEM) supplemented with 10% FBS and 100 U/ml penicillin and 0.1% streptomycin and maintained in 5% CO_2 at 37°C and used for Thy1-scFv binding assays as stated below.

Binding of Thy1-scFv to Thy1-expressing MS1 cells

Biological functionality evaluation of Thy1-scFv to specifically bind cell-surface, $MS1_{WT}$ and $MS1_{Thy1}$ cells were incubated with Thy1-scFv-APC conjugate. Dye conjugation was performed by biotinylation of Thy1-scFv followed by stretavidin-APC incubation following the manufacturer's recommendation. Briefly, Thy1-scFv was incubated with 20-fold molar excess of NHS-PEG4-Biotin (Pierce Biotechnology, Rockford, lL) at room temperature for 30 minutes in PBS. Excess of biotin was removed using a Zeba spin column (Pierce Biotechnology, Rockford, lL) before the addition of streptavidin-APC (Tonbo Biosciences, San Diego, CA) to form Thy1-scFv-APC. Then, $MS1_{WT}$ and $MS1_{Thy1}$ cells were incubated with Thy1-scFv-APC (500 nM) or with a commercial Thy1-Ab-APC (eBioscience Inc, San Diego, CA) for 1 hour at 4°C, washed 3 times with PBS. Fluorescence intensity from the dye-labeled ligands were visualized by flow cytometry (Guava easyCyte; Luminex Corp., Austin, TX) and analyzed using FlowJo software (Becton Dickinson & company).

Synthesis and preparation of MBThy1-scFv as targeted-US contrast agent

Preparation of the US contrast agents, *i.e.,* MBs, is detailed in the Supplementry Materials. Briefly, Thy1-scFv was conjugated to commercial phospholipids by NHS chemistry so that it composes 10% in the final octafluoropropane filled-vesicle, $MB_{Thy1\text{-}scFv}$. A non-targeted control, $MB_{non\text{-}targeted}$, was made with non-functionalized phospholipids and identical amount of octafluoropropane.

Transgenic mouse model of PDAC

The transgenic pancreatic cancer mouse model (Pdx1-$Cre^{tg/+}$; $KRas^{LSL\ G12D/+}$; Ink4a/$Arf^{-/-}$) (n=3), which spontaneously developed foci within 4 to 7 weeks after birth, was used.[25] Correct genotype was validated for all the mice. Tumor diameter ranging between 1.3 and 2.2 mm (mean 1.7 ± 0.4 mm) based on US images were used for the study. Healthy age-matched littermates were used as normal control group (n=3).

***In vivo* US molecular imaging of pancreas**

In vivo US imaging of vascular Thy1 expression in a transgenic mouse model of PDAC and C57BL/6 mice with normal pancreas was performed using two MB constructs ($MB_{Thy1\text{-}scFv}$ and $MB_{non\text{-}targeted}$) by following the protocol reported previously.[24] In brief, a total of 10^8 $MB_{Thy1\text{-}scFv}$ or $MB_{non\text{-}targeted}$ (100 µL) was utilized for intravenous bolus injection *via* tail vein. All *in vivo* imaging studies were performed in contrast mode using a dedicated small animal high resolution US imaging system (Vevo 2100, FUJIFILM VisualSonics, Inc., Toronto, ON, Canada) with the transducer placed over the abdomen of mice, guided by B-mode imaging to detect the target tissue of interest. Contrast mode images were acquired with a 21MHz linear transducer (MS250, VisualSonics; lateral and axial resolution of 165 µm and 75 µm, respectively), and all imaging parameters (focal length, 10 mm; transmit power, 4%; mechanical index, 0.2; dynamic range, 40 dB and a

center frequency of 21MHz) were kept constant during all imaging sessions. A total time of 5 minutes was allowed for MBs to attach their target before binding quantification. To differentiate the acoustic signal owing to MBs attachment to Thy1 and the signal from freely circulating MBs, the previously described destruction-replenishment technique was employed.[22] The protocol consisted of 3 steps: (i) 200 frames of images capturing blood-vessel bound and unbound MBs within the region of interest (ROI), (ii) a high pressure destructive pulse (1- second continuous high-power destructive pulse of 3.7 MPa, transmit power, 100%; mechanical index, 0.63) to destroy all bound and unbound MBs, and (iii) an additional set of 200 frames to measure the signal intensity from the unbound MBs flowing into the ROI immediately after the destructive pulse. The difference in US imaging signal pre- and post-destruction corresponds to the Thy1 attached contrast agents, $MB_{Thy1\text{-}scFv}$ or $MB_{non\text{-}targeted}$. A waiting interval of 20 minutes was maintained between each MB injections to allow for complete clearance before subsequent imaging. Any remaining attached MBs were destroy by applying a high-power destruction pulse (see above for acoustic parameters).

Ultrasound molecular imaging data analysis

The molecular imaging signals were quantified post image acquisition with correction for breathing motion artifacts using Vevo 2100 integrated analysis software (VevoCQ; VisualSonics). Data analysis was accomplished by manually drawing ROIs around PDAC tissues, adjacent non-PDAC tissues, as well as in the normal pancreas of control littermates. The magnitude of imaging signal from attached MBs was assessed by subtracting the average imaging signals pre- and post-destruction, and expressed as the differential targeted enhancement (dTE) in arbitrary units (a.u.).

Ex vivo analysis of pancreas tissues

PDAC mice were euthanized in accordance with animal care guidelines. The pancreas was excised and fixed in 4% paraformaldehyde (Santa Cruz Biotechnology Inc., CA) at 4°C for 24 hours. Tissues were cryosectioned and stained with hematoxylin eosin before analysis using a Nanozoomer (Hamamatsu, Japan).

Statistical Analysis

Student-test was applied to determine statistical significance (**P<0.03; ***P<0.02;) between groups and data expressed as Mean ± SD.

Conflict of Interest: The authors declare no conflict of interest.

Acknowledgments : The authors would like to thank Canary Center at Stanford, Department of Radiology for providing the facility and resources for executing this work.

Source of Funding: This work was funded by Phase I (R41 CA203090) and Phase II SBIR Grants from NIH.

Author contributions: N.J and R.P designed the study; N.J and R.P performed the experiments; N.J, and R.P, were involved in data analysis, R.B helped with *in vivo* imaging; N.J and R.P, wrote the manuscript. All authors reviewed the manuscript.

REFERENCES

1. Chang, A. C. Y.; Cohen, S. N. Genome Construction Between Bacterial Species In Vitro: Replication and Expression of Staphylococcus Plasmid Genes in Escherichia Coli. *Proceedings of the National Academy of Sciences* **1974**, *71* (4), 1030–1034. https://doi.org/10.1073/pnas.71.4.1030.

2. Demain, A. L.; Vaishnav, P. Production of Recombinant Proteins by Microbes and Higher Organisms. *Biotechnology Advances* **2009**, *27* (3), 297–306. https://doi.org/10.1016/j.biotechadv.2009.01.008.

3. Rosano, G. L.; Ceccarelli, E. A. Recombinant Protein Expression in Escherichia Coli: Advances and Challenges. *Front. Microbiol.* **2014**, *5*. https://doi.org/10.3389/fmicb.2014.00172.

4. Swartz, J. R. Advances in Escherichia Coli Production of Therapeutic Proteins. *Current Opinion in Biotechnology* **2001**, *12* (2), 195–201. https://doi.org/10.1016/S0958-1669(00)00199-3.

5. Khow, O.; Suntrarachun, S. Strategies for Production of Active Eukaryotic Proteins in Bacterial Expression System. *Asian Pac J Trop Biomed* **2012**, *2* (2), 159–162. https://doi.org/10.1016/S2221-1691(11)60213-X.

6. Protein Production and Purification. *Nat Methods* **2008**, *5* (2), 135–146. https://doi.org/10.1038/nmeth.f.202.

7. Costa, S.; Almeida, A.; Castro, A.; Domingues, L. Fusion Tags for Protein Solubility, Purification and Immunogenicity in Escherichia Coli: The Novel Fh8 System. *Front. Microbiol.* **2014**, *5*. https://doi.org/10.3389/fmicb.2014.00063.

8. Ritz, D.; Beckwith, J. Roles of Thiol-Redox Pathways in Bacteria. *Annu. Rev. Microbiol.* **2001**, *55* (1), 21–48. https://doi.org/10.1146/annurev.micro.55.1.21.

9. Singh, A.; Upadhyay, V.; Upadhyay, A. K.; Singh, S. M.; Panda, A. K. Protein Recovery from Inclusion Bodies of Escherichia Coli Using Mild Solubilization Process. *Microb Cell Fact* **2015**, *14* (1), 41. https://doi.org/10.1186/s12934-015-0222-8.

10. Bowden, G. A.; Paredes, A. M.; Georgiou, G. Structure and Morphology of Protein Inclusion Bodies in Escherichia Coli. *Nat Biotechnol* **1991**, *9* (8), 725–730. https://doi.org/10.1038/nbt0891-725.

11. Palmer, I.; Wingfield, P. T. Preparation and Extraction of Insoluble (Inclusion-Body) Proteins from Escherichia Coli. *Curr Protoc Protein Sci* **2012**, *0 6*. https://doi.org/10.1002/0471140864.ps0603s70.

12. Singhvi, P.; Saneja, A.; Srichandan, S.; Panda, A. K. Bacterial Inclusion Bodies: A Treasure Trove of Bioactive Proteins. *Trends in Biotechnology* **2020**, *38* (5), 474–486. https://doi.org/10.1016/j.tibtech.2019.12.011.

13. Malhotra, A. Tagging for protein expression. *Methods Enzymol*. **2009,** 463:239-58. http://doi.org/10.1016/S0076-6879(09)63016-0.

14. Pina, A. S.; Lowe, C. R.; Roque, A. C. A. Challenges and Opportunities in the Purification of Recombinant Tagged Proteins. *Biotechnology Advances* **2014**, *32* (2), 366–381. https://doi.org/10.1016/j.biotechadv.2013.12.001.

15. Smyth, D. R.; Mrozkiewicz, M. K.; McGrath, W. J.; Listwan, P.; Kobe, B. Crystal Structures of Fusion Proteins with Large-Affinity Tags. *Protein Sci.* **2003**, *12* (7), 1313–1322. https://doi.org/10.1110/ps.0243403.

16. Sauzay, C.; Voutetakis, K.; Chatziioannou, A.; Chevet, E.; Avril, T. CD90/Thy-1, a Cancer-

Associated Cell Surface Signaling Molecule. *Front. Cell Dev. Biol.* **2019**, *7*. https://doi.org/10.3389/fcell.2019.00066.

17. Croix, B. S.; Rago, C.; Velculescu, V.; Traverso, G.; Romans, K. E.; Montgomery, E.; Lal, A.; Riggins, G. J.; Lengauer, C.; Vogelstein, B.; Kinzler, K. W. Genes Expressed in Human Tumor Endothelium. *Science* **2000**, *289* (5482), 1197–1202. https://doi.org/10.1126/science.289.5482.1197.

18. Madden, S. L.; Cook, B. P.; Nacht, M.; Weber, W. D.; Callahan, M. R.; Jiang, Y.; Dufault, M. R.; Zhang, X.; Zhang, W.; Walter-Yohrling, J.; Rouleau, C.; Akmaev, V. R.; Wang, C. J.; Cao, X.; St. Martin, T. B.; Roberts, B. L.; Teicher, B. A.; Klinger, K. W.; Stan, R.-V.; Lucey, B.; Carson-Walter, E. B.; Laterra, J.; Walter, K. A. Vascular Gene Expression in Nonneoplastic and Malignant Brain. *Am J Pathol* **2004**, *165* (2), 601–608.

19. Chen, X.; Higgins, J.; Cheung, S.-T.; Li, R.; Mason, V.; Montgomery, K.; Fan, S.-T.; Rijn, M. van de; So, S. Novel Endothelial Cell Markers in Hepatocellular Carcinoma. *Mod Pathol* **2004**, *17* (10), 1198–1210. https://doi.org/10.1038/modpathol.3800167.

20. Bradley, J. A.; Ramirez, G.; Hagood, J. S. Roles and Regulation of Thy-1, a Context-Dependent Modulator of Cell Phenotype. *Biofactors* **2009**, *35* (3), 258–265. https://doi.org/10.1002/biof.41.

21. True, L. D.; Zhang, H.; Ye, M.; Huang, C.-Y.; Nelson, P. S.; von Haller, P. D.; Tjoelker, L. W.; Kim, J.-S.; Qian, W.-J.; Smith, R. D.; Ellis, W. J.; Liebeskind, E. S.; Liu, A. Y. CD90/THY1 Is Overexpressed in Prostate Cancer-Associated Fibroblasts and Could Serve as a Cancer Biomarker. *Mod Pathol* **2010**, *23* (10), 1346–1356. https://doi.org/10.1038/modpathol.2010.122.

22. Foygel, K.; Wang, H.; Machtaler, S.; Lutz, A. M.; Chen, R.; Pysz, M.; Lowe, A. W.; Tian, L.; Carrigan, T.; Brentnall, T. A.; Willmann, J. K. Detection of Pancreatic Ductal Adenocarcinoma in Mice by Ultrasound Imaging of Thymocyte Differentiation Antigen 1. *Gastroenterology* **2013**, *145* (4), 885-894.e3. https://doi.org/10.1053/j.gastro.2013.06.011.

23. Zhu, J.; Thakolwiboon, S.; Liu, X.; Zhang, M.; Lubman, D. M. Overexpression of CD90 (Thy-1) in Pancreatic Adenocarcinoma Present in the Tumor Microenvironment. *PLoS One* **2014**, *9* (12). https://doi.org/10.1371/journal.pone.0115507.

24. Abou-Elkacem, L.; Wang, H.; Chowdhury, S. M.; Kimura, R. H.; Bachawal, S. V.; Gambhir, S. S.; Tian, L.; Willmann, J. K. Thy1-Targeted Microbubbles for Ultrasound Molecular Imaging of Pancreatic Ductal Adenocarcinoma. *Clin Cancer Res* **2018**, *24* (7), 1574–1585. https://doi.org/10.1158/1078-0432.CCR-17-2057.

25.Aguirre, A. J.; Bardeesy, N.; Sinha, M.; Lopez, L.; Tuveson, D. A.; Horner, J.; Redston, M. S.; DePinho, R. A. Activated Kras and Ink4a/Arf Deficiency Cooperate to Produce Metastatic Pancreatic Ductal Adenocarcinoma. *Genes Dev* **2003**, *17* (24), 3112–3126. https://doi.org/10.1101/gad.1158703.

26. Vera, A.; González-Montalbán, N.; Arís, A.; Villaverde, A. The Conformational Quality of Insoluble Recombinant Proteins Is Enhanced at Low Growth Temperatures. *Biotechnol. Bioeng.* **2007**, *96* (6), 1101–1106. https://doi.org/10.1002/bit.21218.

27. Singh, A.; Upadhyay, V.; Panda, A. K. Solubilization and Refolding of Inclusion Body Proteins. In *Insoluble Proteins*; García-Fruitós, E., Ed.; Methods in Molecular Biology; Springer New York: New York, NY, 2015; Vol. 1258, pp 283–291. https://doi.org/10.1007/978-1-4939-2205-5_15.

28. Upadhyay, V.; Singh, A.; Jha, D.; Singh, A.; Panda, A. K. Recovery of Bioactive Protein from Bacterial Inclusion Bodies Using

Trifluoroethanol as Solubilization Agent. *Microb Cell Fact* **2016**, *15* (1), 100. https://doi.org/10.1186/s12934-016-0504-9.

29. Raines, R. T.; McCormick, M.; Van Oosbree, T. R.; Mierendorf, R. C. The S·tag Fusion System for Protein Purification. In *Methods in Enzymology*; Academic Press, 2000; Vol. 326, pp 362–376. https://doi.org/10.1016/S0076-6879(00)26065-5.

30. Crimmins, D. L.; Mische, S. M.; Denslow, N. D. Chemical Cleavage of Proteins on Membranes. CurrentProtocols in Protein Science. Copyright by John Wiley & Sons, Inc 2000, 11.5.1–11.5.13. https://doi.org/10.1002/0471140864.ps1105s19.

31. Waugh, D. S. An Overview of Enzymatic Reagents for the Removal of Affinity Tags. *Protein Expression and Purification* **2011**, *80* (2), 283–293. https://doi.org/10.1016/j.pep.2011.08.005.

32. Isetti, G.; Maurer, M. C. Employing Mutants to Study Thrombin Residues Responsible for Factor XIII Activation Peptide Recognition: A Kinetic Study †. *Biochemistry* **2007**, *46* (9), 2444–2452. https://doi.org/10.1021/bi0622120.

33. Bromfield, K. M.; Quinsey, N. S.; Duggan, P. J.; Pike, R. N. Approaches to Selective Peptidic Inhibitors of Factor Xa. *Chem Biol Drug Design* **2006**, *68* (1), 11–19. https://doi.org/10.1111/j.1747-0285.2006.00404.x.

34. Gasparian, M. E.; Ostapchenko, V. G.; Schulga, A. A.; Dolgikh, D. A.; Kirpichnikov, M. P. Expression, Purification, and Characterization of Human Enteropeptidase Catalytic Subunit in Escherichia Coli. *Protein Expression and Purification* **2003**, *31* (1), 133–139. https://doi.org/10.1016/S1046-5928(03)00159-1.

35. Kapust, R. B.; Tözsér, J.; Fox, J. D.; Anderson, D. E.; Cherry, S.; Copeland, T. D.; Waugh, D. S. Tobacco Etch Virus Protease: Mechanism of Autolysis and Rational Design of Stable Mutants with Wild-Type Catalytic Proficiency. *Protein Engineering, Design and Selection* **2001**, *14* (12), 993–1000. https://doi.org/10.1093/protein/14.12.993.

36. Long, A. C.; Orr, D. C.; Cameron, J. M.; Dunn, B. M.; Kay, J. A Consensus Sequence for Substrate Hydrolysis by Rhino Virus 3C Proteinase. *FEBS Letters* **1989**, *258* (1), 75–78. https://doi.org/10.1016/0014-5793(89)81619-9.

37. American Cancer Society. Cancer Facts et Figures 2020. Atlanta: American Cancer Society. 2020

38. Jugniot, N.; Bam, R.; Meuillet, E. J.; Unger, E. C.; Paulmurugan, R. Current Status of Targeted Microbubbles in Diagnostic Molecular Imaging of Pancreatic Cancer. *Bioeng Transl Med* **2021**, *6* (1). https://doi.org/10.1002/btm2.10183.

39. Bam, R.; Daryaei, I.; Abou-Elkacem, L.; Vilches-Moure, J. G.; Meuillet, E. J.; Lutz, A.; Marinelli, E. R.; Unger, E. C.; Gambhir, S. S.; Paulmurugan, R. Toward the Clinical Development and Validation of a Thy1-Targeted Ultrasound Contrast Agent for the Early Detection of Pancreatic Ductal Adenocarcinoma. *Invest Radiol* **2020**, *55* (11), 711–721. https://doi.org/10.1097/RLI.0000000000000697.

Supplementary Files

This is a list of supplementary files associated with this preprint. Click to download.

- SupplementarymaterialsJugniotal..pdf